

Supporting Information

A gap-designed photo-reactor for high-performance photothermal methane reforming

Hamada A. El-Naggar, Hisao Yoshida, and Akira Yamamoto*

Affiliation and full postal address

*Department of Interdisciplinary Environment, Graduate School of Human and Environmental Studies,
Kyoto University, Yoshida Nihonmatsu-cho, Sakyo-ku, Kyoto 606-8501, Japan*

Corresponding authors

Dr. Akira Yamamoto

Department of Interdisciplinary Environment, Graduate School of Human and Environmental Studies,
Kyoto University, Yoshida Nihonmatsu-cho, Sakyo-ku, Kyoto 606-8501, Japan

Tel: +81-75-753-6882

Fax: +81-75-753-2988

E-mail address: yamamoto.akira.2a@kyoto-u.ac.jp

Photograph of the 1-mm-gap reactor



Figure S1 Photograph of the 1-mm-gap reactor filled with 35 mg of $\text{Co}_5\text{Ni}_{95}\text{@SiO}_2$ catalyst.

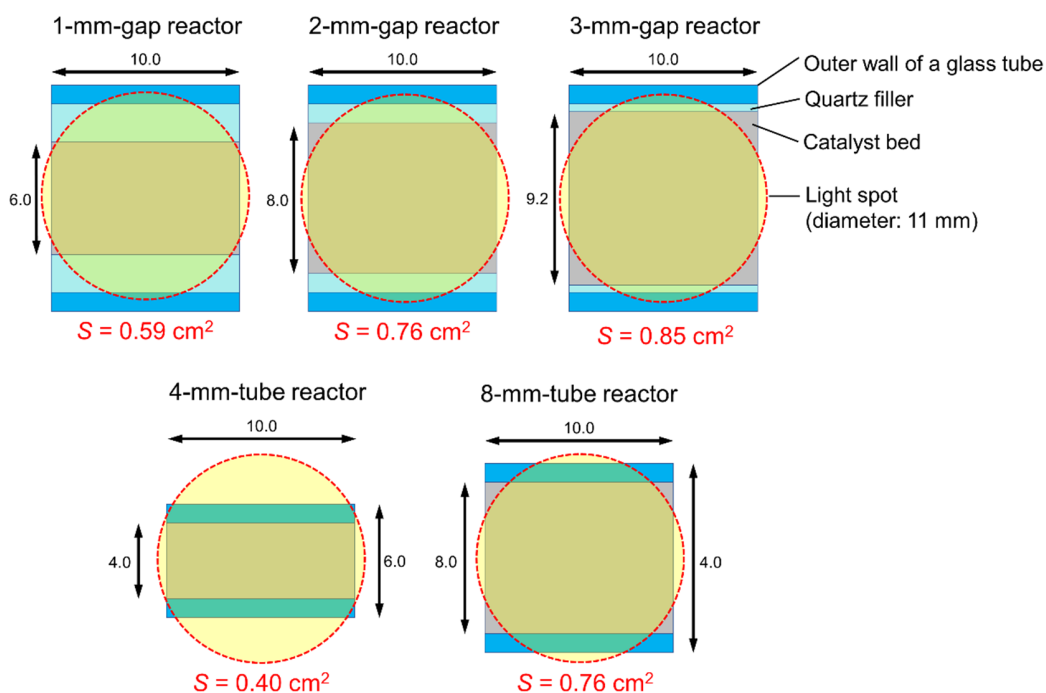


Figure S2 Top view of the reactors under light irradiation with a spot diameter of 11 mm. The cross-sectional area for light absorption (S) was calculated from the overlap between the catalyst zone and the light spot.

Supplementary Note 1

To measure the temperature, we fixed a thin thermocouple (diameter: 0.5 mm) at the back side of the catalyst zone in the 2-mm-gap reactor (i.e., the surface in contact with the quartz filler, center position in the quartz filler). Then, the catalyst was filled into the reactor and was reduced under the same conditions as described in the experimental section in the manuscript. After the catalyst was cooled down, an argon gas was flowed at 200 mL min^{-1} , and the temperature of the backside of the catalyst was recorded under light irradiation ($P = 25 \text{ W}$ and $\Phi = 7 \text{ mm}$). The obtained temperature at the backside was around $723 \text{ }^\circ\text{C}$. Simultaneously, the surface temperature recorded using the IR thermometer was $917 \text{ }^\circ\text{C}$. The results indicated there was a significant difference in the temperature of the surface and backside, supporting our argument that narrowing down the difference between the backside and surface temperatures of the catalyst zone had a positive impact on the performance of the CH_4 reforming.

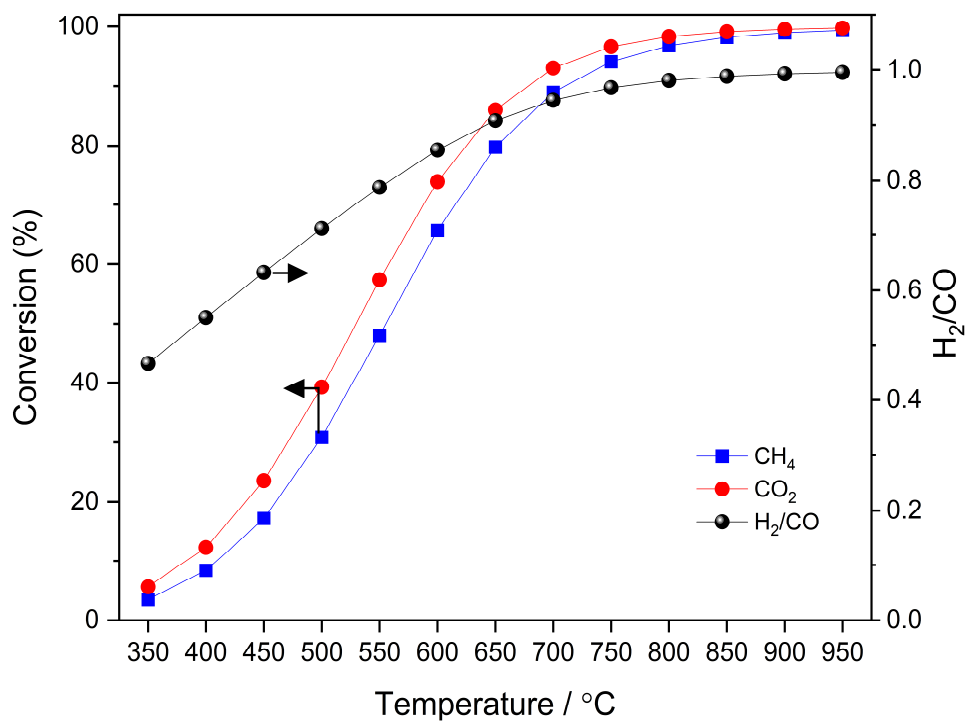


Figure S3 Chemical equilibrium conversion and H₂/CO ratio of DRM reaction calculated by the NASA CEA program.

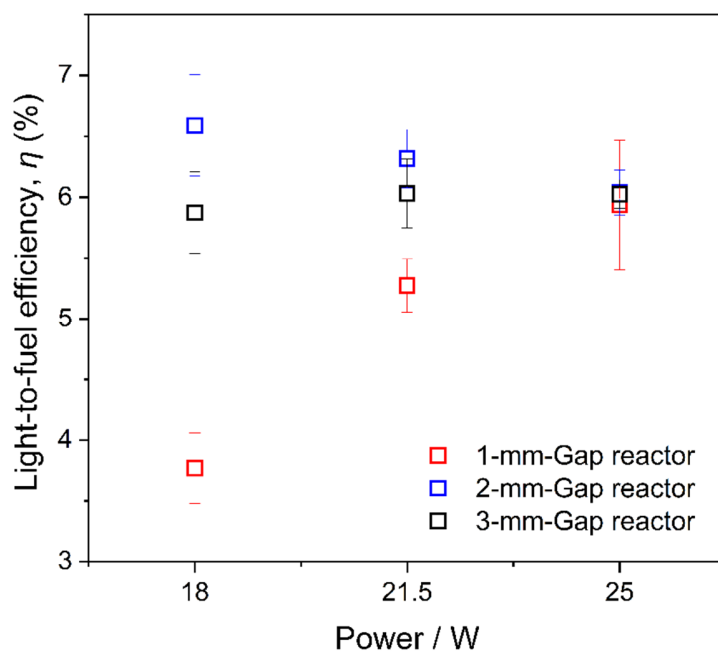


Figure S4 The light-to-fuel conversion efficiency (η) calculated from activity tests using 1-, 2-, and 3-mm-gap reactors (light power: 18, 21.5, and 25 W, and spot size: 11 mm)

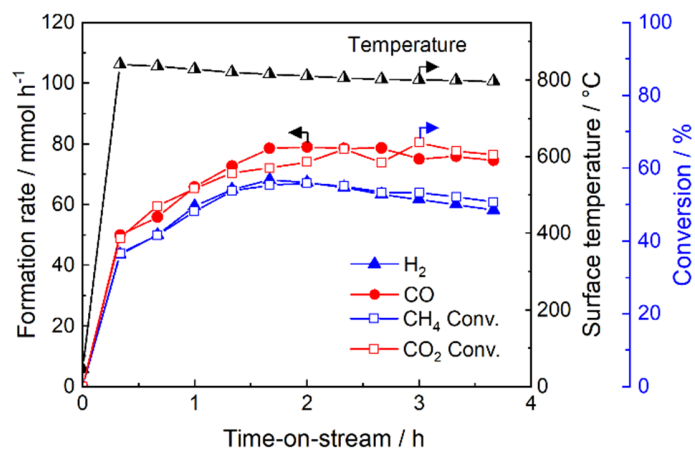


Figure S5 Results of activity test using 4-mm tubular reactor under $P = 25$ W, with Spot diameter = 7 mm, Spot position: Middle.

Table S1 Selected results of light-driven dry reforming of methane without external heating.

Catalyst	Reactor type	Light source	Feed / ^[a] mL min ⁻¹	Conversion (%)		Efficiency (%) ^[b]	Details of light conditions ^[c]	Ref. ^[d]
				CH ₄	CO ₂			
Co ₅ Ni ₉₅ @SiO ₂	Gap reactor, Tube-based,	Xe lamp, 300 W	$F_{\text{CH}_4} = 22.5$ $F_{\text{CO}_2} = 22.5$	72	78	$\eta = 6.0$	$P = 25 \text{ W}$ $\Phi = 7 \text{ mm}$ $I = 650 \text{ kW m}^{-2}$ $\lambda > 435 \text{ nm}$	This work
NiCo/ MgO-Al ₂ O ₃ (Ni/Co = 1)	Stainless-steel cavity reactor	Xe lamp, 300 W	$F_{\text{CH}_4} = (44.4)$ $F_{\text{CO}_2} = (44.7)$	<i>n.d.</i> ^[e] (~55)	<i>n.d.</i> ^[e] (~63)	$\eta = 33.8$	$P = 12.6 \text{ W}$ $\Phi = 6 \text{ mm}$ $I = 445.6 \text{ kW m}^{-2}$ Full spectrum (Xe)	[1]
NiCo@MgO/MgO (Ni/Co = 2)	Stainless-steel cavity reactor	Xe lamp, 500 W	$F_{\text{CH}_4} = 36$ $F_{\text{CO}_2} = 36$	<i>n.d.</i> ^[e] (~40)	<i>n.d.</i> ^[e] (~48)	$\eta = 39.3$	$P = 7.8 \text{ W}$ $\Phi = 5 \text{ mm}$ $I = 396.8 \text{ kW m}^{-2}$ Full spectrum (Xe)	[2]
Co ₅ Ni ₉₅ @SiO ₂	Tube-based reactor	Xe lamp, 300 W	$F_{\text{CH}_4} = 20$ $F_{\text{CO}_2} = 25$	40	41	$\eta = 6.5$	$P = 25 \text{ W}$ $\Phi = 7 \text{ mm}$ $I = 650 \text{ kW m}^{-2}$ $\lambda > 435 \text{ nm}$	[3]
Co/Mg-CoAl ₂ O ₄	Stainless-steel cavity reactor	Xe lamp 500 W	$F_{\text{CH}_4} = (27.2)$ $F_{\text{CO}_2} = (27.7)$	<i>n.d.</i> ^[e] (~37)	<i>n.d.</i> ^[e] (~45)	$\eta = 34.2$	$P = 6.3 \text{ W}$ $\Phi = 10 \text{ mm}$ $I = 80.5 \text{ kW m}^{-2}$ Full spectrum	[4]
Silica-cluster-modified Ni/SiO ₂	Stainless-steel cavity reactor	Xe lamp 500 W	$F_{\text{CH}_4} = (13.9)$ $F_{\text{CO}_2} = (13.7)$	<i>n.d.</i> ^[e] (~37)	<i>n.d.</i> ^[e] (~41)	$\eta = 12.5$	$P = 6.74 \text{ W}$ $\Phi = 5 \text{ mm}$ $I = 343.6 \text{ kW m}^{-2}$ Full spectrum	[5]
Pt/Co-Al ₂ O ₃	Stainless-steel cavity reactor	Xe lamp 500 W	$F_{\text{CH}_4} = (25.7)$ $F_{\text{CO}_2} = (25.8)$	<i>n.d.</i> ^[e] (~35)	<i>n.d.</i> ^[e] (~43)	$\eta = 27.2$	$P = 6.7 \text{ W}$ $\Phi = 5 \text{ mm}$ $I = 343.0 \text{ kW m}^{-2}$ Full spectrum (Xe)	[6]
Rh/SrTiO ₃	Stainless-steel cavity reactor	Hg-Xe lamp, 150 W	$F_{\text{CH}_4} = (0.01)$ $F_{\text{CO}_2} = (0.01)$	<i>n.d.</i> ^[e] (~28)	<i>n.d.</i> ^[e] (~28)	AQE = 5.9	Absorbed photon number: 1.25×10^{17} (quanta cm ⁻² s ⁻¹)	[7]
1.2Ni-0.3Co/SiO ₂	flow type reactor	Xe lamp, 300 W	$F_{\text{CH}_4} = 9.6$ $F_{\text{CO}_2} = 9.6$	-	<i>n.d.</i> ^[e] (~23)	-	$I = 90 \text{ kW m}^{-2}$	[8]
25 wt% Ni/SiO ₂	Tube-based reactor	Xe lamp, 300 W	$F_{\text{CH}_4} = 20$ $F_{\text{CO}_2} = 25$	8.2	7.5	-	$P = 17.3 \text{ W}$ $\Phi = 20 \text{ mm}$ $I = 55 \text{ kW m}^{-2}$ $\lambda > 435 \text{ nm}$	[9]

[a] F : flow rate of CO₂ or CH₄ (mL min⁻¹). [b] η : light-to-fuel conversion efficiency, AQE: apparent quantum efficiency as reported by the authors. [c] Conditions of light irradiation. P : power, Φ : light spot diameter, I : light intensity, and λ : wavelength of light. [d] Reference. [e] No data. The values in parentheses are calculated ones based on the values or Figures in the papers.

References

- [S1] X. Liu, H. Shi, X. Meng, C. Sun, K. Zhang, L. Gao, Y. Ma, Z. Mu, Y. Ling, B. Cheng, Y. Li, Y. Xuan, Y. Ding, Solar-Enhanced CO₂ Conversion with CH₄ over Synergetic NiCo Alloy Catalysts with Light-to-Fuel Efficiency of 33.8%, *Sol. RRL*, 5 (2021) 2100185.
- [S2] S. Wu, G. Ji, P. Qiu, Q. Hu, J. Tian, Y. Li, High Fuel Yields, Solar-to-Fuel Efficiency, and Excellent Durability Achieved for Confined NiCo Alloy Nanoparticles Using MgO Overlayers for Photothermocatalytic CO₂ Reduction, *Sol. RRL*, 6 (2022) 2200369.
- [S3] H.A. El-Naggar, D. Takami, H. Asanuma, T. Hirata, H. Yoshida, A. Yamamoto, Photothermal Dry Reforming of Methane on Yolk-Shell Co–Ni Alloy@SiO₂ Catalyst, *ChemCatChem*, (2024) e202401396.
- [S4] Z. Cui, Q. Hu, Y. Li, J. Wu, X. Yu, H. Cao, L. Ji, M. Zhong, Z. Chen, Synergetic effect for highly efficient light-driven CO₂ reduction by CH₄ on Co/Mg-CoAl₂O₄ promoted by a photoactivation, *Applied Catalysis B: Environment and Energy*, 350 (2024) 123917.
- [S5] H. Huang, M. Mao, Q. Zhang, Y. Li, J. Bai, Y. Yang, M. Zeng, X. Zhao, Solar-Light-Driven CO₂ Reduction by CH₄ on Silica-Cluster-Modified Ni Nanocrystals with a High Solar-to-Fuel Efficiency and Excellent Durability, *Adv. Energy Mater.*, 8 (2018) 1702472.
- [S6] Z. Xie, Y. Li, Z. Zhou, Q. Hu, J. Wu, S. Wu, Significantly enhancing the solar fuel production rate and catalytic durability for photothermocatalytic CO₂ reduction by a synergetic effect between Pt and Co doped Al₂O₃ nanosheets, *J. Mater. Chem. A*, 10 (2022) 7099-7110.
- [S7] S. Shoji, X. Peng, A. Yamaguchi, R. Watanabe, C. Fukuhara, Y. Cho, T. Yamamoto, S. Matsumura, M.-W. Yu, S. Ishii, T. Fujita, H. Abe, M. Miyauchi, Photocatalytic uphill conversion of natural gas beyond the limitation of thermal reaction systems, *Nat. Catal.*, 3 (2020) 148-153.
- [S8] J. Zhang, K. Xie, Y. Jiang, M. Li, X. Tan, Y. Yang, X. Zhao, L. Wang, Y. Wang, X. Wang, Y. Zhu, H. Chen, M. Wu, H. Sun, S. Wang, Photoinducing Different Mechanisms on a Co-Ni Bimetallic Alloy in Catalytic Dry Reforming of Methane, *ACS Catal.*, 13 (2023) 10855-10865.
- [S9] D. Takami, J. Tsubakimoto, W. Sarwana, A. Yamamoto, H. Yoshida, Photothermal Dry Reforming of Methane over Phyllosilicate-Derived Silica-Supported Nickel Catalysts, *ACS Applied Energy Materials*, 6 (2023) 7627-7635.